Supporting Information

Negative sulfur-based electrodes and their application in battery cells: Dual-ion batteries as an example

Verena Küpers[1], Martin Kolek[1], Peter Bieker[1,2], Marian Cristian Stan[1]*, Tobias Placke[1], Martin Winter[1,2]*

1 MEET Battery Research Center, Institute of Physical Chemistry
University of Münster
Corrensstraße 46, 48149 Münster, Germany
2 Helmholtz Institute Münster (HI MS), IEK-12
Forschungszentrum Jülich GmbH
Corrensstrasse 46, 48149 Münster, Germany

Email:
Marian Cristian Stan
marian.stan@uni-muenster.de

Martin Winter
m.winter@fz-juelich.de

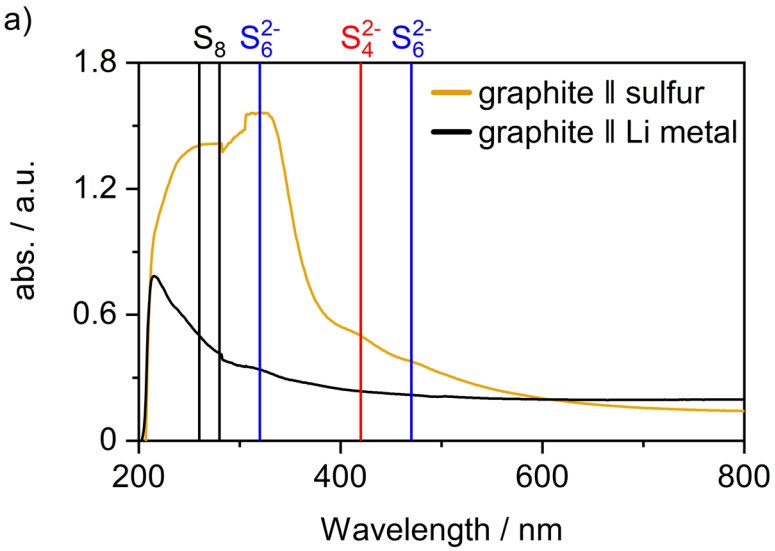

Figure S1. UV/vis spectra of the electrolytes (diluted in 1,2-Dimethoxyethane (DME)) after an initial charge at 10 mA g^{-1} in graphite ‖ sulfur (WE ‖ CE, yellow) and graphite ‖ Li metal (WE ‖ CE, black) Swagelok T-cells (three-electrode configuration, half-cell setup) with 1 M LiTFSI in Pyr_{14}TFSI (Li-Pyr) electrolyte and a Li metal ($Li|Li^+$) RE at 20 °C. The cut-off potentials (WE) were set to 5.0 V *vs*. $Li|Li^+$. The graphite ‖ sulfur cell did not reach the cut-off potential and was stopped after a time restriction of 10 hours. The adsorption maxima of the UV/vis spectra and the assigned PSs (S_8, S_6^{2-} and S_4^{2-}) are indicated based on *Bieker et al*.[1].

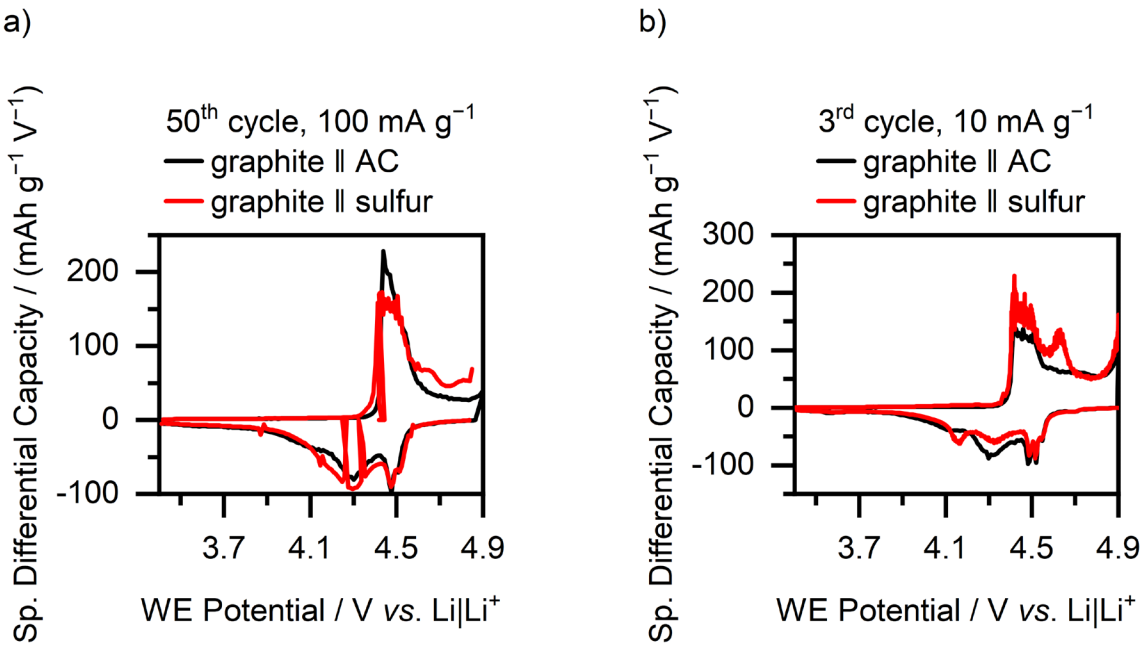

Figure S2. Specific differential capacity *vs*. potential plots of a) the 50th cycle at 100 mA g^{-1} and b) the 3rd cycle at 10 mA g^{-1} of graphite ‖ sulfur (WE ‖ CE) and graphite ‖ AC (WE ‖ CE; black, data taken from ref. [2], published under the terms of a CC BY 4.0 license, https://creativecommons.org/licenses/by/4.0/) Swagelok T-cells (three-electrode configuration, half-cell setup) with 1 M LiTFSI in $Pyr_{14}TFSI$ (Li-Pyr) electrolyte and a Li metal (Li|Li$^+$) RE at 20 °C and cut-off potentials of 3.4 and 4.9 V *vs*. Li|Li$^+$ for the graphite WE and additional limits of 1.5 and 3.0 V *vs*. Li|Li$^+$ for the sulfur CE (only for the graphite ‖ sulfur cells).

a) Pristine graphite electrode (WE)

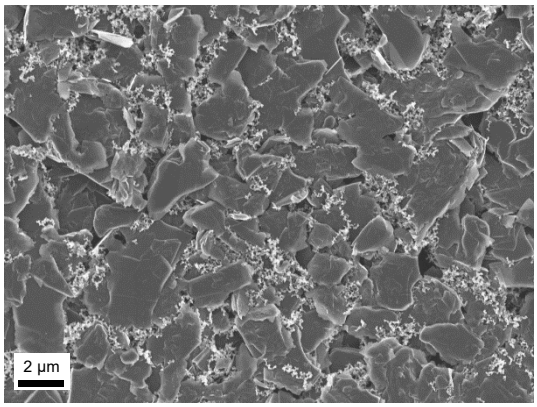

b) Pristine sulfur electrode (CE)

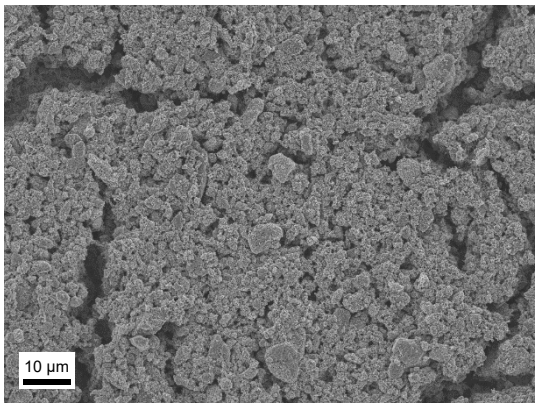

c) CE cycled in a graphite ‖ sulfur cell

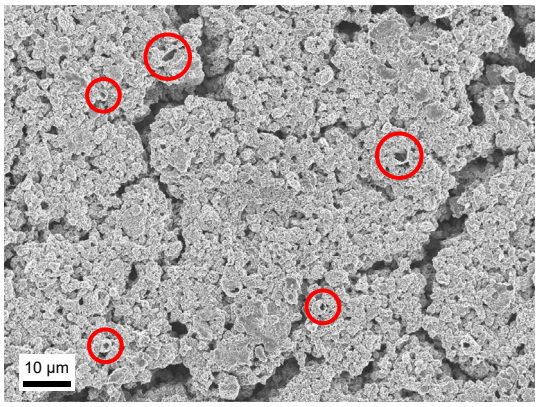

Figure S3. SEM images of a) a pristine graphite WE (5000x magnification), b) a pristine sulfur CE (1000x magnification) and c) a CE after three full cycles (3.4 to 4.9 V vs. $Li|Li^+$) and one charge to 4.9 V vs. $Li|Li^+$ at 10 mA g^{-1} in graphite ‖ sulfur (WE ‖ CE) Swagelok T-cells (three-electrode configuration, half-cell setup) with 1 M LiTFSI in $Pyr_{14}TFSI$ (Li-Pyr) electrolyte and a Li metal ($Li|Li^+$) RE at 20 °C (1000x magnification). The potential of the CE in the graphite ‖ sulfur cells was additionally limited to 1.5 and 3.0 V *vs*. $Li|Li^+$.

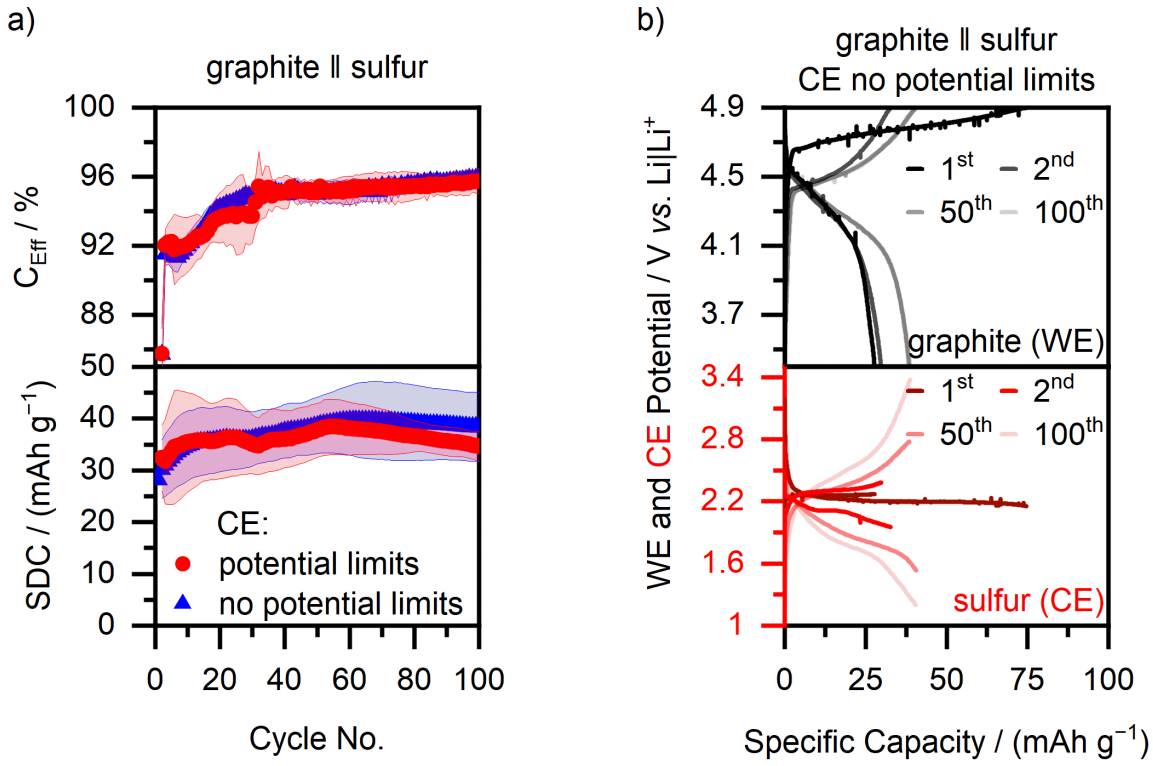

Figure S4. a) C_{Eff}s and SDCs of graphite ‖ sulfur (WE ‖ CE) Swagelok-type cells (three-electrode configuration, half-cell setup) with 1 M LiTFSI in $Pyr_{14}TFSI$ (Li-Pyr) electrolyte and a Li metal (Li|Li$^+$) RE at 20 °C, 100 mA g^{-1} (10 mA g^{-1} in the 1st cycle) and cut-off potentials of 3.4 and 4.9 V *vs.* Li|Li$^+$ for the WE and additional limits of 1.5 and 3.0 V *vs.* Li|Li$^+$ for the CE (red) or without additional limits for the CE (blue). b) The corresponding potential profiles of the WE (graphite, black) and CE (sulfur, red) of the graphite ‖ sulfur cell with not potential limited CE at the 1st, 2nd, 50th and 100th cycle. The C_{Eff}s of the first cycle (CE with potential limits: 41 ± 2%; CE without potential limits: 38 ± 2%) are not shown.

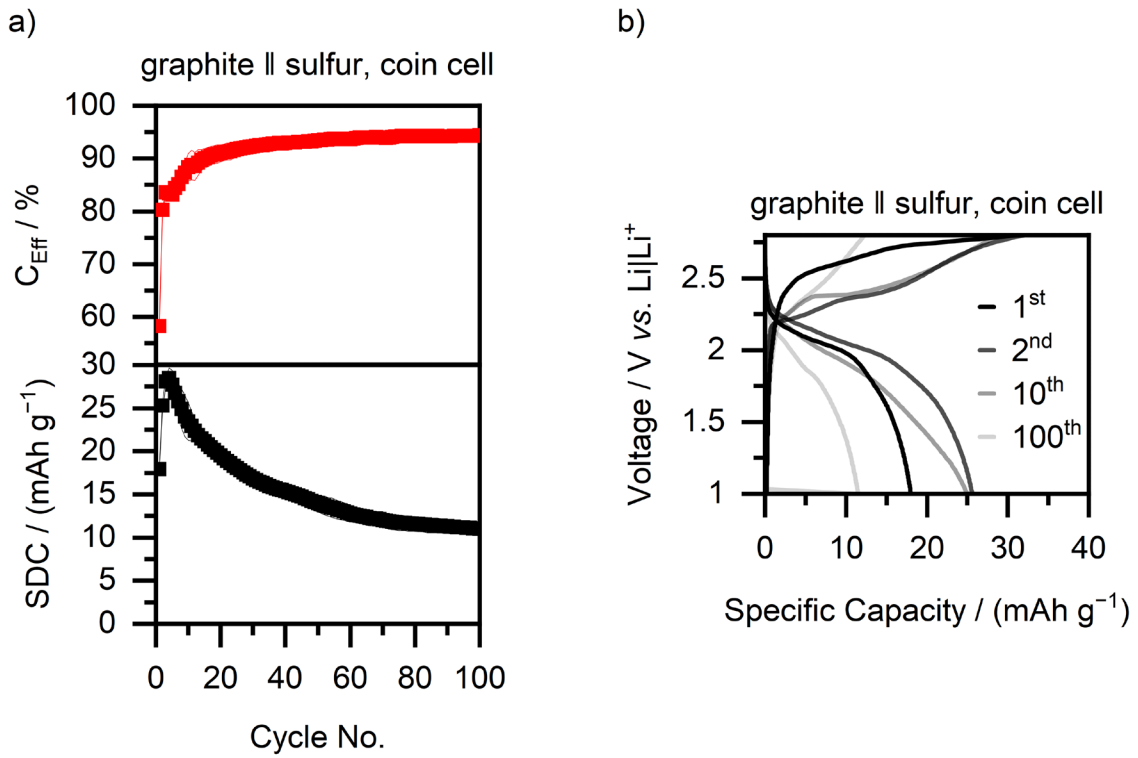

Figure S5. C_{Eff}s and SDCs of graphite ‖ sulfur (P ‖ N) coin cells (two-electrode configuration) with 1 M LiTFSI in Pyr_{14}TFSI (Li-Pyr) electrolyte at 100 mA g^{-1} and cut-off potentials of 1 and 2.8 V. b) The corresponding voltage profiles at the 1st, 2nd, 10th and 100th cycle.

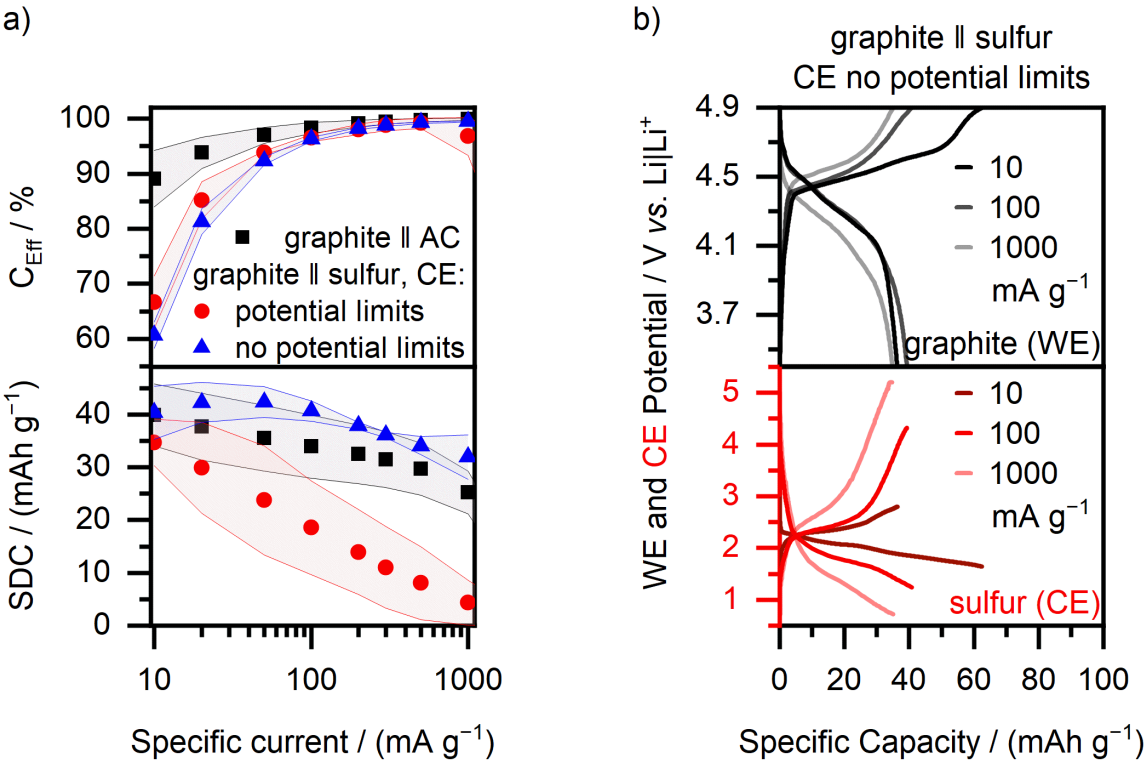

Figure S6. a) C_{Eff}s and SDCs of graphite ‖ sulfur (WE ‖ CE; red and blue) and graphite ‖ AC (WE ‖ CE; black, data taken from ref. [2], published under the terms of a CC BY 4.0 license, https://creativecommons.org/licenses/by/4.0/) Swagelok-type cells (three-electrode configuration, half-cell setup) with 1 M LiTFSI in Pyr_{14}TFSI (Li-Pyr) electrolyte and a Li metal (Li|Li$^+$) RE at various specific currents. The cut-off potentials at all currents were fixed to 3.4 and 4.9 V *vs.* Li|Li$^+$ for the WE with additional limits of 1.5 and 3.0 V *vs.* Li|Li$^+$ for the CE (only red). b) The corresponding potential profiles of the WE (graphite) and CE (sulfur) of the graphite ‖ sulfur cell without limits for the CE (blue in a)) at 10, 100 and 1000 mA g^{-1}.

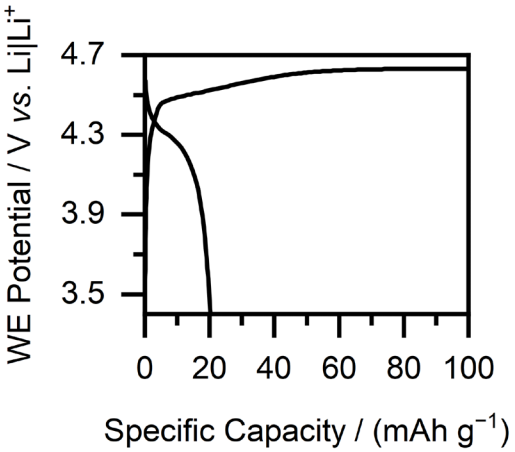

Figure S7. WE potential profile of graphite ‖ sulfur (WE ‖ CE) cells with 7 mol kg^{-1} LiTFSI in DME at 100 mA g^{-1} and 20 °C (1st cycle).

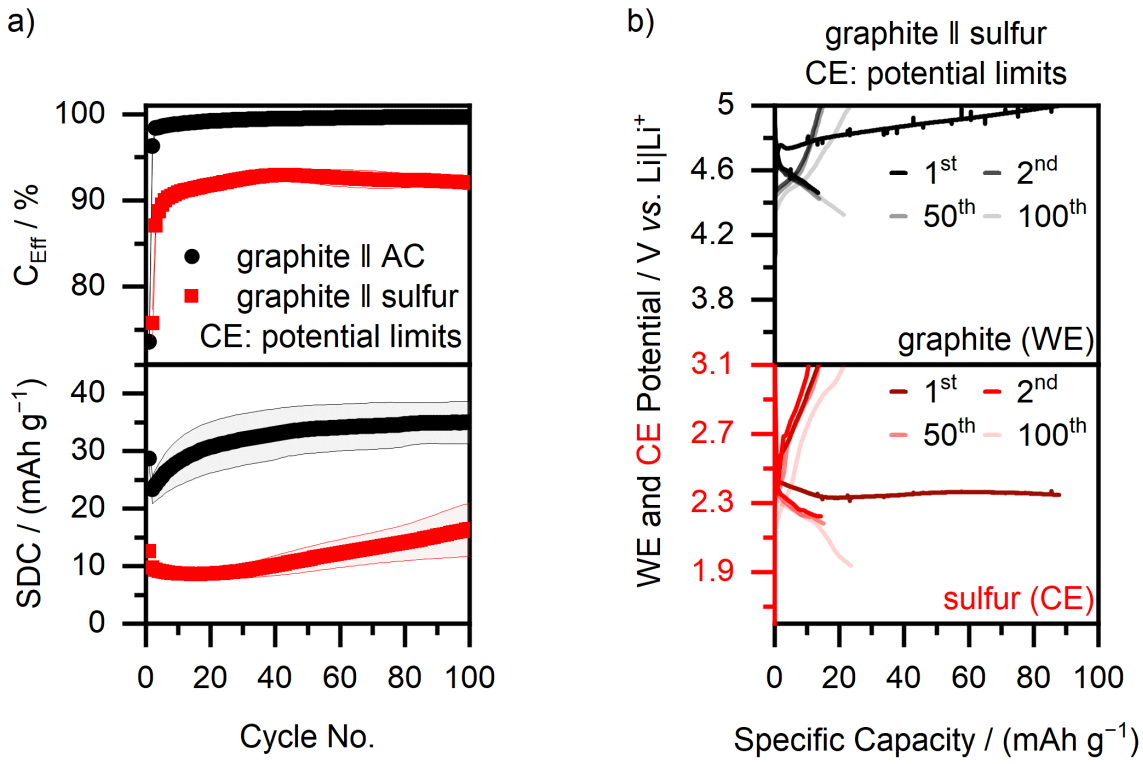

Figure S8. a) C_{Eff}s and SDCs of graphite ‖ sulfur (WE ‖ CE; red) and graphite ‖ AC (WE ‖ CE; black, data taken from ref. [2], published under the terms of a CC BY 4.0 license, https://creativecommons.org/licenses/by/4.0/) Swagelok-type cells (three-electrode configuration, half-cell setup) with 0.5 M $Mg(TFSI)_2$ in $Pyr_{14}TFSI$ (Mg-Pyr) electrolyte and a Li metal (Li|Li$^+$) qRE at 20 °C, 100 mA g^{-1} (10 mA g^{-1} in the 1st cycle) and cut-off potentials of 3.4 and 5.0 V *vs.* Li|Li$^+$ for the WE and additional limits of 1.6 and 3.1 V *vs.* Li|Li$^+$ for the CE (only for the graphite ‖ sulfur cells). b) The corresponding potential profiles of the WE (graphite, black) and CE (sulfur, red) at the 1st, 2nd, 50th and 100th cycle. The C_{Eff}s of the first cycle (CE = AC: 74 ± 1%[2]; CE = sulfur: 15.2 ± 0.1%) are not shown.

a) WE cycled in a graphite ‖ sulfur cell

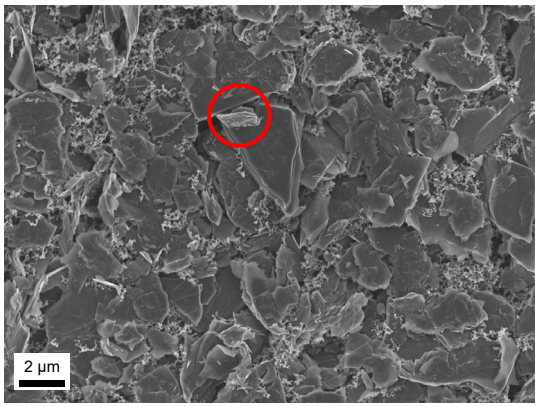

b) WE cycled in a graphite ‖ AC cell

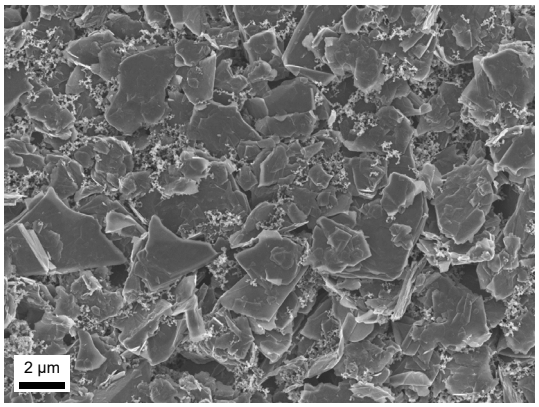

c) CE cycled in a graphite ‖ sulfur cell

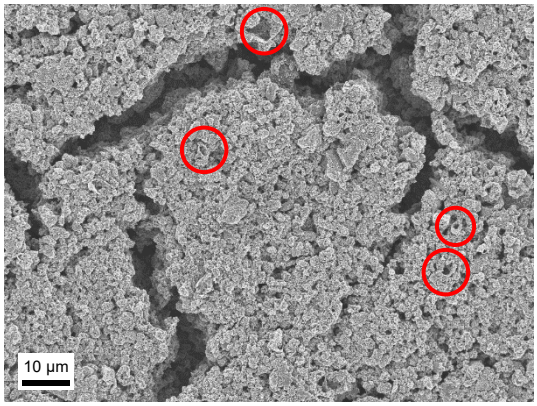

Figure S9. SEM images of graphite a) and b) WEs (5000x magnification) and c) a CE after three full cycles (3.4 to 4.9 V vs. Li|Li$^+$) and one charge to 4.9 V vs. Li|Li$^+$ at 10 mA g^{-1} in a) and c) graphite ‖ sulfur (WE ‖ CE) and b) graphite ‖ AC (WE ‖ CE) Swagelok-type cells (three-electrode configuration, half-cell setup) with 1 M LiTFSI in $Pyr_{14}TFSI$ (Li-Pyr) electrolyte and a Li metal (Li|Li$^+$) RE at 20 °C. The potential of the CE in the graphite ‖ sulfur cells was additionally limited to 1.6 and 3.1 V *vs*. Li|Li$^+$. The SEM image of pristine graphite and sulfur electrodes is given in **Figure S2a** and **b**.

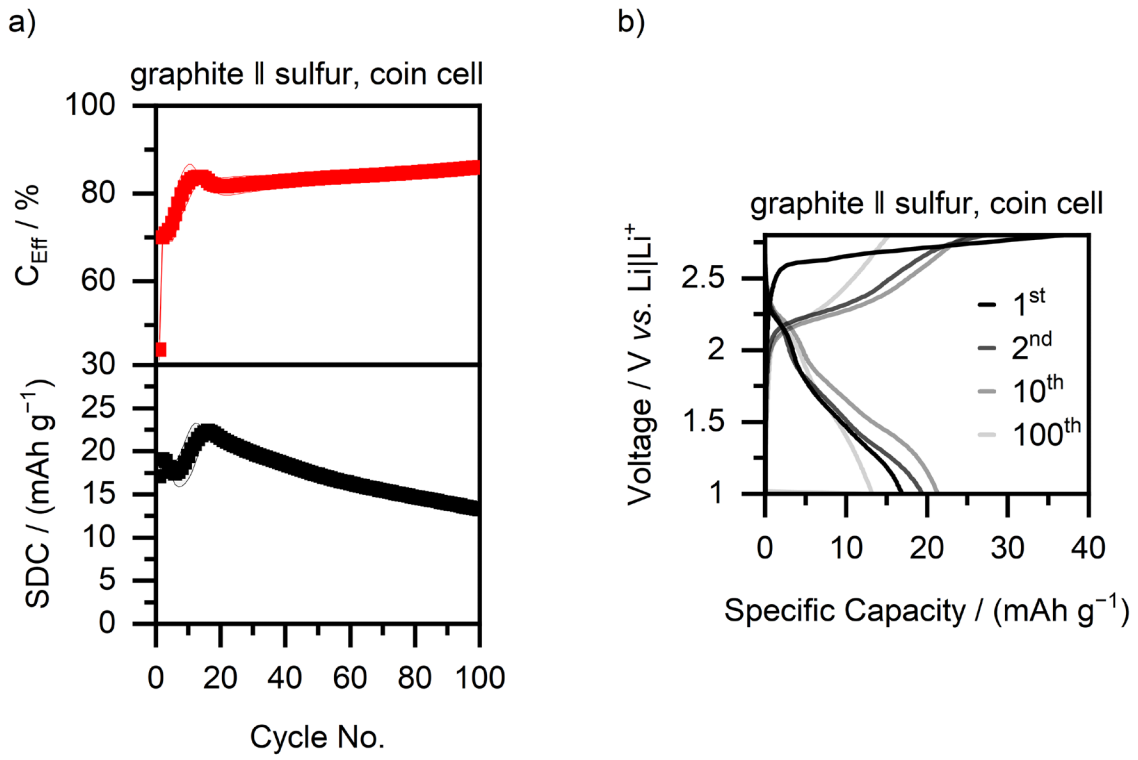

Figure S10. C_{Eff}s and SDCs of graphite ‖ sulfur (P ‖ N) coin cells (two-electrode configuration) with 0.5 M $Mg(TFSI)_2$ in $Pyr_{14}TFSI$ (Mg-Pyr) electrolyte at 100 mA g^{-1} and cut-off potentials of 1 and 2.8 V. b) The corresponding voltage profiles at the 1st, 2nd, 10th and 100th cycle.

Table S1. The element amounts (C, O, F, S) in atomic % (at. %) and the F:S ratio determined by EDX spectroscopy of the WEs and CEs in the pristine state after three full cycles (3.4 to 4.9 V vs. Li|Li$^+$) and one charge to 4.9 V vs. Li|Li$^+$ at 10 mA g^{-1} in graphite ‖ sulfur (WE ‖ CE) and graphite ‖ AC (WE ‖ CE) Swagelok-type cells (three-electrode configuration, half-cell setup) with 1 M LiTFSI in $Pyr_{14}TFSI$ (Li-Pyr) electrolyte and a Li metal (Li|Li$^+$) RE. The potential of the CE in the graphite ‖ sulfur cells was additionally limited to 1.5 and 3.0 V *vs*. Li|Li$^+$. The amounts of further elements (Al, Na, Co, W) contained in the inactive materials (current collector, binder and conductive carbons) are not displayed.

WE	**C / at. %**	**O / at. %**	**F / at. %**	**S / at. %**	**F:S ratio**
Pristine grapite electrode	96.6 ± 0.3	2.6 ± 0.6	-	-	-
graphite ‖ sulfur	95.0 ± 0.1	2.2 ± 0.2	1.8 ± 0.2	1.0 ±0.1	1.8:1
graphite ‖ AC	92 ± 2	2.9 ± 0.8	4 ± 1	1.1 ± 0.2	3.5:1
CE	**C / at. %**	**O / at. %**	**F / at. %**	**S / at. %**	**F:S ratio**
Pristine sulfur electrode	85.4 ± 0.4	5 ± 2	-	8 ± 3	-
graphite ‖ sulfur	87 ± 4	5 ± 2	3 ± 3	4 ± 1	<1:1

Table S2. The element amounts (C, O, F, S) in atomic % (at. %) and the F:S ratio determined by EDX spectroscopy of the WEs and CEs in the pristine state after three full cycles (3.4 to 5.0 V vs. Li|Li$^+$) and one charge to 5.0 V vs. Li|Li$^+$ at 10 mA g^{-1} in graphite ‖ sulfur (WE ‖ CE) and graphite ‖ AC (WE ‖ CE) Swagelok-type cells (three-electrode configuration, half-cell setup) with 0.5 M $Mg(TFSI)_2$ in $Pyr_{14}TFSI$ (Mg-Pyr) electrolyte and a Li metal (Li|Li$^+$) RE. The potential of the CE in the graphite ‖ sulfur cells was additionally limited to 1.6 and 3.1 V *vs*. Li|Li$^+$. The amounts of further elements (Al, Na, Co, W) contained in the inactive materials (current collector, binder and conductive carbons) are not displayed.

WE	**C / at. %**	**O / at. %**	**F / at. %**	**S / at. %**	**F:S ratio**
Pristine grapite	96.6 ± 0.3	2.6 ± 0.6	-	-	-
graphite ‖ sulfur	95.1 ± 0.9	1.9 ± 0.4	1.7 ± 0.4	1.3 ± 0.1	1.4:1
graphite ‖ AC	92 ± 2	3.0 ± 0.8	4.0 ± 0.9	1.1 ± 0.2	3.7:1
CE	**C / at. %**	**O / at. %**	**F / at. %**	**S / at. %**	**F:S ratio**
Pristine sulfur electrode	85.4 ± 0.4	5 ± 2	-	8 ± 3	-
graphite ‖ sulfur	85.6 ± 0.6	6 ± 2	2.9 ± 0.8	3.0 ± 0.1	<1:1

Table S3. SDCs and C_{Eff}s of the 1st, 2nd, 10th, 50th, and 100th cycle of graphite ‖ AC (WE ‖ CE; black, data taken from ref. [2], published under the terms of a CC BY 4.0 license, https://creativecommons.org/licenses/by/4.0/) and graphite ‖ sulfur (WE ‖ CE) Swagelok-type cells (three-electrode configuration, half-cell setup) with 1 M LiTFSI (Li-Pyr) and 0.5 M $Mg(TFSI)_2$ (Mg-Pyr) in $Pyr_{14}TFSI$, and a Li metal ($Li|Li^+$) quasi reference electrode. The cells were cycled at 20 °C (unless stated otherwise), 100 mA g^{-1} (10 mA g^{-1} in the 1st cycle) and cut-off potentials of 3.4 and 4.9 V (Li-Pyr) or 5.0 V (Mg-Pyr) *vs*. $Li|Li^+$ for the WE and additional limits of 1.5 to 3.0 V (Li-Pyr), respectively 1.6 to 3.1 V *vs*. $Li|Li^+$ (Mg-Pyr) for the CE (only for selected graphite ‖ sulfur cells).

	graphite ‖ AC, Li-Pyr[2]		**Graphite ‖ sulfur, Li-Pyr WE:CE = 1:6, CE = no potential limits**		**Graphite ‖ sulfur, Li-Pyr WE:CE = 1:6, CE = potential limits**	
	SDCs / mAh g^{-1}	**C_{Eff} / %**	**SDCs / mAh g^{-1}**	**C_{Eff} / %**	**SDCs / mAh g^{-1}**	**C_{Eff} / %**
1st cycle	32 ± 1	64 ± 2	28 ± 2	38 ±2	26 ± 2	41 ± 2
2nd cycle	31 ± 3	95.6 ± 0.4	30 ± 6	86 ± 2	28 ± 6	86 ± 2
10th cycle	35 ± 4	98.2 ± 0.5	35 ± 7	92.0 ± 0.7	33 ± 8	92 ± 2
50th cycle	37 ± 4	99.1 ± 0.3	39 ± 5	95.0 ± 0.6	37 ± 5	95.1 ± 0.7
100th cycle	36 ± 3	99.3 ± 0.2	38 ± 7	95.9 ± 0.3	33 ± 3	95.8 ± 0.7

	graphite ‖ sulfur, Li-Pyr WE:CE = 1:6, CE = potential limits, 60 °C	
	SDCs / mAh g^{-1}	**C_{Eff} / %**
1st cycle	0.5 ± 0.2	0.5 ± 0.2
2nd cycle	41 ± 20	27 ± 13
10th cycle	30 ± 16	38 ± 16

	graphite ‖ AC, Mg-Pyr[2]		**graphite ‖ sulfur, Mg-Pyr WE:CE = 1:6, CE = no potential limits**		**graphite ‖ sulfur, Mg-Pyr WE:CE = 1:6, CE = potential limits**	
	SDCs / mAh g^{-1}	**C_{Eff} / %**	**SDCs / mAh g^{-1}**	**C_{Eff} / %**	**SDCs / mAh g^{-1}**	**C_{Eff} / %**
1st cycle	29 ± 1	74 ± 1	31 ± 3	54 ± 3	12.6 ± 0.7	15.2 ± 0.1
2nd cycle	23 ± 2	96.3 ± 0.3	28 ± 3	89.6 ± 0.5	9.8 ± 0.7	76 ± 2
10th cycle	28 ± 4	98.9 ± 0.3	33 ± 3	94 ± 1	8.7 ± 0.6	90.9 ± 0.3
50th cycle	34 ± 4	99.5 ± 0.1	36 ± 2	95.0 ± 0.9	11 ± 2	92.8 ± 0.8
100th cycle	35 ± 4	99.7 ± 0.1	36 ± 6	95 ± 1	17 ± 5	92.1 ± 0.9

Table S4. SDCs and C_{Eff}s of graphite ‖ AC (WE ‖ CE; black, data taken from ref. [2], published under the terms of a CC BY 4.0 license, https://creativecommons.org/licenses/by/4.0/) and graphite ‖ sulfur (WE ‖ CE) Swagelok-type cells (three-electrode configuration, half-cell setup) with 1 M LiTFSI in Pyr_{14}TFSI (Li-Pyr) and a Li metal ($Li|Li^+$) quasi reference electrode. The cells were cycled at 20 °C with various currents from 10 to 1000 mA g^{-1} after one cycle at 10 mA g^{-1} and 30 cycles at 100 mA g^{-1} (the 5th cycle of each specific current is displayed) with cut-off potentials of 3.4 and 4.9 V *vs*. $Li|Li^+$ for the WE and additional limits of 1.5 to 3.0 V *vs*. $Li|Li^+$ for the CE (only for selected graphite ‖ sulfur cells).

	graphite ‖ AC, Li-Pyr[2]		**graphite ‖ sulfur, Li-Pyr WE:CE = 1:6 CE = no potential limits**		**graphite ‖ sulfur, Li-Pyr WE:CE = 1:6 CE = potential limits**	
Current / mA g^{-1}	**SDCs / mAh g^{-1}**	**C_{Eff} / %**	**SDCs / mAh g^{-1}**	**C_{Eff} / %**	**SDCs / mAh g^{-1}**	**C_{Eff} / %**
10	40 ± 6	89 ± 5	40 ± 5	61 ± 2	35 ± 4	67 ± 5
20	38 ± 6	94 ± 3	42 ± 4	81 ± 2	30 ± 9	85 ± 3
50	36 ± 6	97 ± 1	42 ± 3	92.3 ± 0.7	24 ± 10	93.8 ± 0.3
100	34 ± 6	98 ± 1	41 ± 2	96.3 ± 0.4	19 ± 9	96.5 ± 0.6
200	33 ± 6	99.1 ± 0.6	37.9 ± 0.7	98.2 ± 0.2	14 ± 8	98.0 ± 0.9
300	31 ± 5	99.4 ± 0.4	36.2 ± 0.5	98.8 ± 0.2	11 ± 8	99 ± 1
500	30 ± 5	99.7 ± 0.3	34 ± 2	99.3 ± 0.1	8 ± 7	99.2 ± 0.9
1000	25 ± 4	99.9 ± 0.2	32 ± 4	99.5 ± 0.1	4 ± 4	97 ± 3

References

1. Bieker G, Wellmann J, Kolek M, Jalkanen K, Winter M, Bieker P (2017). Influence of cations in lithium and magnesium polysulphide solutions: dependence of the solvent chemistry. Phys. Chem. Chem. Phys. 19:11152-11162
2. Küpers V, Dohmann JF, Bieker P, Winter M, Placke T, Kolek M (2021). Opportunities and Limitations of Ionic Liquid- and Organic Carbonate Solvent-Based Electrolytes for Mg-Ion-Based Dual-Ion Batteries. ChemSusChem 14:4480-4498